

JAAS

Accepted Manuscript



This is an *Accepted Manuscript*, which has been through the Royal Society of Chemistry peer review process and has been accepted for publication.

Accepted Manuscripts are published online shortly after acceptance, before technical editing, formatting and proof reading. Using this free service, authors can make their results available to the community, in citable form, before we publish the edited article. We will replace this *Accepted Manuscript* with the edited and formatted *Advance Article* as soon as it is available.

You can find more information about *Accepted Manuscripts* in the [Information for Authors](#).

Please note that technical editing may introduce minor changes to the text and/or graphics, which may alter content. The journal's standard [Terms & Conditions](#) and the [Ethical guidelines](#) still apply. In no event shall the Royal Society of Chemistry be held responsible for any errors or omissions in this *Accepted Manuscript* or any consequences arising from the use of any information it contains.

Rapid Size Characterization of Silver Nanoparticles by Single Particle ICP-MS and Isotope Dilution

L. Telgmann,^a C.D. Metcalfe^b and H. Hintelmann^{a,b*}

Trent University, Water Quality Centre, 1600 West Bank Drive, Peterborough, Ontario, K9J 7B8, Canada. ^a Department of Chemistry. ^b Environmental and Resource Studies.

* corresponding author

ABSTRACT

The increasing application of silver nanoparticles (AgNP) in consumer products and their potential release into the environment call for intensive investigation of their toxicity, stability, and fate. Analytical methods that are able to detect and characterize AgNPs at low concentrations and in complex matrices are needed. Single particle inductively coupled plasma mass spectrometry (spICP-MS) has in recent years emerged to a reliable technique suitable to quantify and size nanoparticles at low concentrations. However, the size determination by means of spICP-MS depends on external calibration with nanoparticle or element standard solutions. Here, a new approach is introduced using internal calibration with isotope dilution to determine the size of different AgNPs. External calibration becomes unnecessary, leading to a more rapid nanoparticle characterization and more robustness towards matrix effects.

The power of the method is shown by determining the size of 50 nm citrate capped and 80 nm PVP capped AgNPs spiked with ¹⁰⁹Ag enriched silver standard. The method is highly reproducible and shows good agreement with results obtained by established methods. The successful size determination of AgNPs in wastewater and river water using this method demonstrates its practicability even in samples with high matrix loads.

Sample preparation only requires the addition of an isotope enriched standard, which makes the method interesting for long-term studies when AgNPs have to be characterized on many different days. As an example, the size alteration of AgNPs under different conditions was monitored over a period of four days, employing the developed method of internal calibration with isotope dilution.

34 Introduction

35
36 The use of nanomaterials in consumer products has increased tremendously in the past years.
37 Silver nanoparticles (AgNP) are integrated into a wide range of products for antibacterial
38 purposes, including socks, bandages, food containers, washing machines, deodorants, and
39 refrigerators. Typically, AgNPs have a structure with a silver Ag(0) core of varying size and
40 shape, and an organic coating with varying molecular weight and functional groups. These
41 surface capping agents, such as polyvinylpyrrolidone (PVP) or citrate, stabilize the
42 nanoparticles and inhibit aggregation.¹

43 AgNPs released from domestic and industrial sources will for the most part enter sewer
44 systems, where they will be carried to wastewater treatment plants.² There is evidence that a
45 high proportion of silver is removed during wastewater treatment.³ Due to the high affinity of
46 silver for sulphur, the AgNPs may be transformed into silver sulphide (Ag₂S) and
47 subsequently incorporated into sewage sludge.^{4,6} However, there have been few published
48 data to show whether all AgNPs are removed during sewage treatment and how much silver is
49 released into the aquatic environment.⁵ The release of AgNP and/or their transformation
50 products into the environment could have impacts on aquatic organisms and human health. It
51 is imperative to monitor the fate of these nanomaterials in wastewater and in the aquatic
52 environment.

53 The analysis of AgNPs and other nanoparticles has in the past been carried out employing a
54 variety of instruments and methods, including transmission electron microscopy (TEM),^{7,8}
55 energy dispersive X-ray spectroscopy (EDX),^{9,10} ultrafiltration,¹¹ asymmetric flow field-flow
56 fractionation (AF4)¹²⁻¹⁴ and reverse phase liquid chromatography (RPLC)¹⁵ with subsequent
57 quantification by inductively coupled plasma mass spectrometry (ICP-MS), to name a few.
58 However, poor detection limits of these methods, laborious sample preparation or
59 susceptibility towards complex matrices such as wastewater prohibited the analysis of
60 samples with low AgNP concentrations in typical environmental samples.

61 Single particle (sp) ICP-MS is an emerging analytical technique that allows not only
62 quantification and sizing of nanoparticles, but also the simultaneous quantification of the
63 respective dissolved metal. In sp mode, nanoparticles are introduced into the ICP-MS
64 individually and are detected as one time-resolved peak for each particle. The intensity of the
65 respective peaks gives information about the particle size, the number of peaks gives
66 information about the particle concentration. At the same time, dissolved silver is detected as
67 a constant signal and can therefore be distinguished from the particle signal.

1
2
3 68 The feasibility of spICP-MS for the analysis of colloids, including titanium and aluminum
4 69 suspensions, was first proposed by Degueldre *et al.* in 2003.¹⁶ Subsequent studies by these
5 70 researchers described the concept in more experimental detail and developed particle
6 71 quantification and sizing techniques.¹⁶⁻¹⁸ Engineered nanoparticles, including silver,^{11,20-31}
7 72 gold,^{20,24,29,30} titanium oxide,²⁷ cerium oxide,²⁷ and zinc oxide²⁷ have since been characterized
8 73 successfully using this analytical approach.

9 74 The size determination of the respective nanoparticles can be carried out using aqueous
10 75 standards of nanoparticles with well-defined diameters. However, not all nanoparticles are
11 76 available in the necessary range of sizes or as mono-dispersed material. Pace *et al.* introduced
12 77 a new sizing method using ordinary element standards of dissolved metals to create an
13 78 external calibration curve.²³ By including parameters such as nanoparticle transport efficiency,
14 79 dwell time, and sample uptake rate into the calculations, the nanoparticle mass and size can be
15 80 determined by relating the signal intensity of the nanoparticle peaks to the external calibration
16 81 curve.²³

17 82 To the best of our knowledge, all strategies described in the literature to determine the size of
18 83 nanoparticles in aqueous solutions are based on external calibrations using standards prepared
19 84 from either nanoparticles or dissolved metals. This can be problematic when measuring
20 85 samples in complex matrices like wastewater, as the analyte response may depend on the
21 86 matrix resulting in inaccurately calculated concentrations. When determining concentrations
22 87 of dissolved analytes, this problem can be avoided by several quantification strategies. One
23 88 common approach to compensate for matrix effects is by isotope dilution analysis (IDA).³²

24 89 The present study describes the application of the IDA approach using ¹⁰⁹Ag for determining
25 90 the size of AgNPs in aqueous matrices by means of spICP-MS. As proof of principle, the
26 91 mass and diameter of AgNPs were determined with conventional external calibration and
27 92 compared to results obtained with internal calibration after spiking with ¹⁰⁹Ag. This new
28 93 method was applied to characterize AgNPs spiked into the influent and effluent of a
29 94 wastewater treatment plant and in river water. In addition, the IDA approach was used to
30 95 monitor changes in the size and concentration of AgNP aged in water over 4 days.

31 96

32 97 **Experimental**

33 98

34 99 **Chemicals and consumables**

35 100 Suspensions of AgNPs with spherical shape and diameters of 50 nm and 80 nm, respectively,
36 101 were purchased from nanoComposix (San Diego, CA, USA). The particles were coated with

1
2
3 102 citrate (50 nm) or PVP (80 nm) capping agent. The suspensions were stabilized with 378
4 103 mg/L citrate and 1-3 $\mu\text{g/L}$ PVP, respectively. Aqueous Ag(I) standard for ICP-MS (1000
5 104 mg/L) was obtained from SPC Science (Baie D'Urfé, QC, Canada). ^{109}Ag (99.4%) enriched
6 105 silver was purchased in metallic form from Isoflex (San Francisco, CA, USA). Nitric acid
7 106 (65%) was purchased from BDH Chemicals through VWR International (Radnor, PA, USA).
8 107 Nylon membrane syringe filters (45 μm) were also obtained from VWR International. All
9 108 chemicals were used in the highest quality available. Water was purified with a Milli-Q
10 109 Element system (Millipore, Billerica, MA, USA).
11 110

111 **Stock and standard solutions**

112 A 1000 mg/L stock solution of ^{109}Ag was prepared by dissolution of 50 mg of the isotope
113 enriched metal in 50 mL of 4% nitric acid. The stock solution was subsequently diluted to a
114 100 $\mu\text{g/L}$ working solution. A working suspension of AgNPs with a concentration (c_{Ag}) of
115 20 $\mu\text{g/L}$ was freshly made every day by dilution of the nanoComposix stock suspension with
116 water. The Ag ICP-MS standard solution was diluted to a 100 $\mu\text{g/L}$ working solution.

117 **Sampling**

118 Grab samples of wastewater (influent and effluent) were collected in July 2013 during dry
119 weather at the wastewater treatment plant for the city of Peterborough, ON, Canada. The plant
120 serves a population of approximately 75,000 people and uses secondary treatment with
121 activated sludge. A grab sample of Otonabee River water was taken from the river bank in
122 July 2013 during dry weather. All samples were collected in polyethylene (PE) bottles and
123 were stored in darkness at 4°C.
124

125 **Instrumentation and set-up**

126 **Transmission Electron Microscope (TEM).** Measurements were carried out with a Philips
127 CM200 TEM. This unit is equipped with a LaB₆-cathode thermionic gun. Operating voltage
128 was set to 200 kV, the point-to-point resolution was 0.24 nm and the line resolution 0.17 nm.
129 Data were evaluated optically/manually from the photomicrographs obtained from the Gatan
130 CCD camera (2k x 2k).

131 **Inductively coupled plasma mass spectrometry (ICP-MS).** A ThermoFisher (Bremen,
132 Germany) XSeries 2 ICP-MS was used for spICP-MS analysis. The samples were introduced
133 into the plasma with a borosilicate glass conical nebulizer (1 ml/min, AHF, Tübingen,
134 Germany) *via* a conical spray chamber with impact bead (AHF). Prior to measurements, the
135 operating conditions were optimized with Ag(I) ICP-MS standard (5 $\mu\text{g/L}$) to maximize the

1
2
3 136 signal intensity. Standard measurements were carried out using the self-aspiration mode of the
4
5 137 nebulizer. The nebulizer gas flow was set to 0.85 L/min. Environmental samples are
6
7 138 transported with a peristaltic pump and mixed in-line with standard solution *via* a T-piece
8
9 139 prior to introduction into the plasma. In this case the nebulizer gas flow was set to 0.93 L/min.
10
11 140 The plasma was run at a RF power of 1450 W. Cool gas was operated with a flow of 15
12
13 141 L/min. The spray chamber was cooled externally to 4°C. The run time was 300 s for AgNP
142
143 suspensions and dissolved Ag(I) solutions.

144 **Sample preparation and experiments**

145 **TEM.** TEM analysis was carried out with undiluted nanoComposix stock suspensions (50 nm,
146
147 80 nm). Prior to measurement, copper TEM grids were soaked in the suspensions and then
148
149 dried.

150 **spICP-MS general.** The size determination with external calibration as well as with isotope
151
152 dilution requires the determination of the particle transport efficiency. A suspension of 80 nm
153
154 PVP capped AgNPs with a defined concentration (i.e. 200 ng/L) was prepared in water. The
155
156 suspension was analyzed every three to four hours in sp mode. This run was also used to
157
158 determine the isotopic abundances and ratios of ^{107}Ag and ^{109}Ag in the nanoparticles. The
159
160 isotope abundance of Ag in the spike solution was also determined daily. A 5 µg/L solution of
161
162 the ^{109}Ag enriched spike was prepared in water. Three replicates of the solutions were
163
164 recorded in sp mode. The exact flow rate of the nebulizer was also determined daily, both for
165
166 uptake with self-aspiration and uptake *via* the T-piece and peristaltic pump. During analyses
167
168 of all samples and calibration solutions and suspensions, the intensities of ^{107}Ag and ^{109}Ag
169
170 were recorded in the same run. The respective quadrupole settling time is 1.9 ms, leading to
171
172 an actual runtime of about 109 s per isotope per run.

173 **Dwell time optimization.** A range of dwell times from 1 - 100 ms have been reported in the
174
175 literature for spICP-MS measurements. Three dwell times of 1 ms, 5 ms, and 10 ms were
176
177 tested for best performance. A suspension of 200 ng/L AgNPs (80 nm, PVP coated) was
178
179 analyzed three times at each dwell time, respectively.

180 **Isotope spiking of AgNPs in water.** To investigate the feasibility of isotope spiking,
181
182 suspensions were prepared in water of 100 ng/L 50 nm citrate capped AgNPs and 200 ng/L 80
183
184 nm PVP capped AgNPs. The 50 nm suspension was spiked with 100 ng/L of ^{109}Ag enriched
185
186 silver and the 80 nm suspension was spiked with 250 ng/L of the isotope enriched Ag. These
187
188 concentrations ensure a ^{109}Ag intensity that is high enough to obtain a measurable difference
189
190 in intensity between the two isotopes needed for IDA, and at the same time allowing definite

170 peak identification in spite of increased signal noise. The spiked suspensions were analyzed
171 ten times in sp mode consecutively. The procedure was repeated on a different day with
172 freshly prepared suspensions to obtain two independent sets of analyses. For the conventional
173 sizing approach using external calibration, Ag(I) standard solutions were made by diluting the
174 working solution to $c_{\text{Ag}} = 0, 0.10, 0.25, 0.50, 0.75, 1.00$ and $2.00 \mu\text{g/L}$.

175 **Wastewater and river water.** Samples of wastewater and river water were filtered through
176 $0.45 \mu\text{m}$ nylon syringe filters. Then, aliquots of the 80 nm PVP capped AgNP working
177 suspension were added to the samples to reach a final nominal concentration of approximately
178 3 mg/L . Separately, a 250 ng/L ^{109}Ag enriched solution (i.e. spike solution) was prepared in
179 water. A T-piece was employed to allow mixing of the sample and spike solution directly
180 before introduction into the ICP-MS. The sample was pumped through tubing with a diameter
181 of 0.38 mm and the spike solution was pumped through tubing with a diameter of 1.85 mm .
182 The peristaltic pump was set on 5 rpm , resulting in a rate of uptake of the sample of $q = 0.21$
183 mL/min and a rate of uptake of the spike solution of $q = 3.29 \text{ mL/min}$. In addition to spiking
184 the sample with isotope enriched standards, this set-up allows dilution of the sample without
185 laborious sample preparation and without altering the sample prior to analysis.

186 **Stability monitoring.** The stability of PVP coated AgNPs (100 ng/L , 80 nm) was monitored
187 over four days under different conditions. Sample 1 and sample 2 were prepared in purified
188 water and stored at room temperature and at 4°C , respectively. Sample 3 was prepared in
189 purified water with a pH of 4.1 , adjusted with nitric acid, and was also stored at room
190 temperature. Samples were run frequently over 4 days in sp mode using the previously
191 described conditions. Directly before measurement, a 5 mL aliquot of the samples was mixed
192 with 5 mL of a 500 ng/L ^{109}Ag standard solution.

193

194 **ICP-MS data acquisition and processing**

195 Data from the ICP-MS were processed using PlasmaLab software, version 2.5.9.300
196 (ThermoFisher). Raw data were exported as Thermo Electron Glitter Format V1.1. The
197 numerical results were subsequently imported into the software OriginLab8 (OriginLab Corp.,
198 Northampton, MA, USA) for further processing.

199 For the determination of mean peak intensities of the AgNPs, ^{107}Ag and ^{109}Ag intensities were
200 plotted as histograms with increments of 1000 cps for measurement with a dwell time of 5 ms
201 (500 cps increment for 10 ms and 2000 cps increment for 1 ms dwell time). The histograms
202 were then in the respective intensity range fitted to a Gaussian function to determine the mean
203 intensity of the nanoparticles in the samples.

1
2
3 204 The mean background intensity was determined by plotting ^{107}Ag and ^{109}Ag intensities with
4
5 205 an increment of 200 cps, and proceeded as described above. The increment was chosen to be
6
7 206 lower, because the intensity of the ^{107}Ag background usually ranges between 0 and 3000 cps,
8
9 207 depending on the age of the sample.

10 208 The mean intensities of the Ag(I) solutions used for external calibration, isotope ratio
11
12 209 determination with Ag ICP-MS standard and ^{109}Ag spike were determined by averaging the
13
14 210 single readings from each analysis.
15

211

212 **Results and Discussion**

213

214 **TEM**

215 TEM measurements yielded an average diameter of 50.2 nm for the 50 nm nanoparticles and
216
217 80.65 nm for the 80 nm nanoparticles. The photomicrographs shown in Figure 1 clearly
218
219 illustrate that the size distribution is very high, which is consistent with the manufacturer's
220
221 information. Also, the AgNPs are not perfectly spherical. This is important since spICP-MS
might work with any NP shape, but the mathematical processing mainly refers to spherical
NPs.

222 **Dwell time optimization**

223 Figure 2 shows the histograms of the peak intensities of the 80 nm PVP capped AgNPs
224
225 analyzed with dwell times of 1 ms, 5 ms, and 10 ms, respectively. The mean intensities of the
226
227 particles are highest for measurements carried out with a dwell time of 1 ms. However, the
228
229 histograms show that the lower minimum of the intensity distribution is not clearly defined,
230
231 and the distribution could not be fitted to a Gaussian function. Most likely, the low dwell time
232
233 prohibits the ICP-MS from detecting the entire ion cloud for each single particle in individual
234
235 data acquisition. The histogram of the measurement carried out with a dwell time of 10 ms
236
237 shows a low mean intensity, but there is a clear minima for the intensity distribution (Figure
2). A second smaller peak at approximately twice the intensity of the main peak, suggests
frequent particle coincidence. This could be avoided by diluting suspensions to lower particle
concentrations, which would mean higher run times to achieve statistically evaluable intensity
distributions.

235 Measurement with a dwell time of 5 ms led to a high mean intensity of the particles (Figure
236
237 2). The histogram indicates infrequent coincidences and a distribution that can easily be fitted
to a Gaussian function. Therefore, for all subsequent measurements, a dwell time of 5 ms was

238 used. The limit of detection regarding particle size under these conditions is 40 nm. This is
239 adequate for the conducted size determination of 50 nm and 80 nm AgNPs, as well as the
240 stability monitoring of 80 nm particles over a couple of days.

241

242 **Size determination of AgNPs in purified water**

243 The transient signal intensity for the 200 ng/L 80 nm AgNPs suspension in water is displayed
244 in Figure 3. Histograms of binned intensities of ^{107}Ag and ^{109}Ag are also shown. Fitting the
245 histograms to a Gaussian function generated mean intensities for both peaks.

246 The background intensity (dissolved silver concentrations) has to be subtracted to avoid
247 inaccurate calculations. For ^{107}Ag measurements, the mean background is easily determined
248 by fitting a Gaussian curve to the background intensity distribution, as described in the
249 experimental section (Data processing). However, determining the background of the ^{109}Ag
250 signal is not straightforward, because the constant silver signal is mainly derived from the
251 dissolved ^{109}Ag spike. Therefore, the ^{109}Ag background was calculated by multiplying the
252 value of the ^{107}Ag background with the ratio of silver natural isotopic abundances
253 ($^{109}\text{Ag}/^{107}\text{Ag}$), determined daily. This procedure is based on the assumption that the
254 background silver contamination is of natural isotope abundance (only possible if the
255 abundance of the spiked enriched isotope is close to 100%), leading to a ^{107}Ag background
256 signal that is slightly higher than the ^{109}Ag background.

257 The following IDA calculations are based on Equation 1. The derivation of this
258 equation (symbols are described below) is described in detail by Rodríguez-González *et al.*³²

259

$$260 \quad c_s = c_{sp} * \frac{m_{sp}}{m_s} * \frac{M_s}{M_{sp}} * \frac{A_{sp}^b}{A_s^a} * \left(\frac{R_m - R_{sp}}{1 - R_m * R_c} \right) \quad (\text{Eq1})$$

261

262 Equation 1 can be used to determine the unknown concentration of a dissolved analyte (c_s)
263 based on the concentration of a dissolved standard of an enriched isotope of the respective
264 analyte (c_{sp}). In our experiments, we used a dissolved standard of ^{109}Ag . However, the aim is
265 to determine the mass of the AgNPs. Therefore, a calculation has to be integrated that
266 correlates the concentration of the dissolved analyte to a total analyte mass per reading.

267 Pace *et al.* developed a protocol for determining the particle mass by using external
268 calibration with dissolved standards.²³ Equation 2 shows how the mass per particle (m_p) can be
269 calculated from the respective analyte concentration introducing transport efficiency η , dwell
270 time dt , and sample uptake rate q as additional parameters.

271

$$m_p = \eta * q * dt * c_s \quad (\text{Eq2})$$

273

274 An increase of the transport efficiency generally leads to a higher signal of the dissolved
 275 analyte, whereas the nanoparticle signal does not change when detected individually
 276 (however, increased transport efficiency would increase the number of measured particles).
 277 Pace *et al.* describe in detail, how Equation 2 accounts for the differences in mass delivery of
 278 dissolved analyte and nanoparticles.²³

279 Equation 1 and equation 2 can now be combined to determine the mass per particle m_p based
 280 on IDA.

281

$$m_p = \eta * q * dt * c_{sp} * \frac{m_{sp}}{m_s} * \frac{M_s}{M_{sp}} * \frac{A_{sp}^b}{A_s^a} * \left(\frac{R_m - R_{sp}}{1 - R_m * R_s} \right) \quad (\text{Eq3})$$

283

284 The concentration of the enriched isotope spike is c_{sp} . The values m_{sp} and m_s are the mass of
 285 the sample and the spike respectively. A_{sp}^b represents the isotopic abundance of ^{109}Ag in the
 286 spike (i.e. 0.994) and A_s^a represents the isotopic abundance of ^{107}Ag in the original sample. A_{sp}^b
 287 and A_s^a are calculated with inputs of the isotope ratio, determined by analyzing daily a fresh
 288 AgNP suspension and the 5 $\mu\text{g/L}$ spike solution, as described in the experimental section.
 289 This procedure circumvents mass discrimination effects which otherwise could cause major
 290 errors in the calculation. M_s is the atomic weight of Ag in the sample and M_{sp} is the atomic
 291 weight of Ag in the spike. The isotope ratio in the mixture of sample and spike is R_m , which is
 292 the ratio of the mean ^{107}Ag and ^{109}Ag nanoparticle peak intensities (background corrected).
 293 R_{sp} is the isotope ratio $^{107}\text{Ag}/^{109}\text{Ag}$ in the spike and R_s is the isotope ratio for $^{109}\text{Ag}/^{107}\text{Ag}$ in
 294 the unspiked sample. The ratios are determined daily by measuring the intensities of both
 295 silver isotopes in a fresh AgNP suspension and a spike solution as described above.

296 The transport efficiency η can be calculated with Equation 4.²³ For the present study, η was
 297 determined daily with the frequency f of AgNP peaks in this run, the sample uptake rate q ,
 298 and the known particle concentration c_p in the AgNP suspension.

299

$$\eta = \frac{f}{q * N_p} \quad (\text{Eq4})$$

301

302 Assuming a spherical geometry, Equation 5 can be used to calculate the particle diameter
 303 from the determined particle mass, using the known density of silver, $\rho = 1.049 \times 10^{-14} \mu\text{g}/\text{nm}^3$.

304

$$d = \sqrt[3]{\frac{6m}{\pi\rho}} \quad (\text{Eq5})$$

306

307 The following example shows the calculations in four steps used for one of the replicate
308 analyses of the 80 nm PVP AgNP suspension:

309

310 Step 1:

- 311 • Determine mean ^{107}Ag and ^{109}Ag intensities of nanoparticle peak by Gaussian fitting

$$312 \quad \text{int. } ^{107}\text{Ag} = 117800 \text{ cps}$$

$$313 \quad \text{int. } ^{109}\text{Ag} = 147500 \text{ cps}$$

- 314 • Determine mean background intensity of ^{107}Ag by Gaussian fitting

$$315 \quad \text{bckg. } ^{107}\text{Ag} = 1500 \text{ cps}$$

- 316 • Background correction

$$317 \quad \text{int. } ^{107}\text{Ag} = 117800 \text{ cps} - 1500 \text{ cps} = 116300 \text{ cps}$$

$$318 \quad \text{int}^{109}\text{Ag} = 147500 \text{ cps} - 1500 \text{ cps} * 0.968 = 146050 \text{ cps}$$

319

320 Step 2:

- 321 • Calculate η by employing Equation 4

$$322 \quad f = 23.367 \text{ particles / s}$$

$$323 \quad q = 0.0215 \text{ mL / s}$$

$$324 \quad c_P = 71051 \text{ particles / mL}$$

$$325 \quad \eta = 0.015$$

- 326 • Determine R_m

$$327 \quad R_m = 116300 \text{ cps} / 146050 \text{ cps} = 0.796$$

- 328 • Determine R_{sp} and R_s

$$329 \quad R_{sp} = 0.006$$

$$330 \quad R_s = 0.968$$

331

332 Step 3:

- 333 • Calculate the particle mass by employing Equation 3

$$334 \quad m_P = 2.811 \times 10^{-9} \mu\text{g}$$

335

336 Step 4:

- 1
2
3 337 • Calculate the particle diameter by employing Equation 5

4 338
$$m = 79.98 \text{ nm}$$

5
6 339

7
8 340 The results of the measurements of the 80 nm PVP-capped and the 50 nm citrate-capped
9 341 AgNPs in water are summarized in Table 1. Results for the silver mass and the diameter of
10 342 the AgNPs are shown for analyses using both our new method using an enriched isotope spike
11 343 as an internal standard and the conventional method using external calibration as described by
12 344 Pace *et al.*²³

13
14
15 345 Relative standard deviations (RSD) between replicate measurements were low (<1.6%) for
16 346 the measurements with internal calibration. Therefore, the new quantitation procedure was
17 347 highly reproducible for calculating the size of AgNPs. More importantly, there was little
18 348 discrepancy between the nanoparticle sizes determined by the new method and by the
19 349 established external calibration method. We assume that the little remaining deviation is
20 350 mostly attributed to small variations in transport efficiency or small inaccuracies in the
21 351 Gaussian fitting of the intensity histograms. Since the RSDs of the results of the new method
22 352 and the method based on external calibration are similar, we propose that the employment of
23 353 the enriched isotope spike does not lead to additional uncertainty in the size determination.

24
25
26 354 The excellent correlation between both methods suggests that spiking with ¹⁰⁹Ag enriched
27 355 silver is well suited for AgNP sizing. Also, these measurements were consistent with the
28 356 mean diameters determined by TEM.

29
30
31 357 One difference between conventional isotope dilution analysis of dissolved elements and that
32 358 of nanoparticles is homogeneity. When detecting metal ions in solution, one can easily
33 359 determine the ratio of two isotopes although they are (usually) determined consecutively with
34 360 a short settling time in between individual isotope mass measurements. In sp mode, however,
35 361 each data reading represents the intensity of one particular NP. Since the NPs vary in mass,
36 362 consecutively measured ¹⁰⁷Ag and ¹⁰⁹Ag signals represent two different particles, which are
37 363 not necessarily of similar size. It is therefore very important to collect sufficient data of
38 364 multiple NPs to allow adequate averaging of peak intensities. Only then a correct
39 365 determination of the mean isotope ratio of AgNPs can be ensured.

40
41
42 366 The fact that consecutively measured ¹⁰⁷Ag and ¹⁰⁹Ag signals represent two different particles
43 367 also prohibits the determination of the isotope ratio of individual NPs. It is therefore difficult
44 368 to determine the size distribution in a solution of nanoparticles with the presented new
45 369 approach. In a suspension of NPs with different sizes, the various mean diameters can only be

46
47
48
49
50
51
52
53
54
55
56
57
58
59
60

1
2
3 370 determined if the maxima in the intensity distribution can be fitted with distinct Gaussian
4 371 curves.

5
6 372

7
8 373 **Wastewater and river water**

9
10 374 Samples in aqueous matrices should be altered as little as possible to avoid potential
11 375 transformation of the analyte. In the case of the AgNPs on hand, dilution should be avoided to
12 376 prevent dissolution of the particles. For this reason, wastewater and river water samples for
13 377 this experiment were only filtered and spiked with AgNPs. As described in the experimental
14 378 section, a T-piece was employed to mix the sample flow with the ^{109}Ag spike solution directly
15 379 before entering the ICP-MS. The respective uptake rates of sample and spike led to a dilution
16 380 factor of ~ 20 .

17
18 381 Particle mass, particle volume and diameter of AgNPs were calculated for spiked (80 nm
19 382 PVP-capped) water and wastewater samples as described above. The mean diameters of
20 383 AgNPs determined from 10 replicate measurements of spiked wastewater influent, effluent,
21 384 and river water sample are presented in Table 2.

22
23 385 The relative standard deviations between replicate measurements were $< 1.9\%$. The new
24 386 procedure for sizing nanoparticles by spiking with isotope enriched silver was highly
25 387 reproducible, even in complex wastewater matrices. The mean calculated sizes showed only a
26 388 slight deviation from the expected value of 80 nm. This approach offers a powerful alternative
27 389 to characterize AgNP rapidly, without additional calibration solutions and without matrix
28 390 interferences.

29
30 391 AgNP concentrations in wastewater and river water were determined by counting NP peaks in
31 392 each run. With the knowledge of transport efficiency η , sample uptake rate q , and dilution
32 393 factor, the particle and corresponding Ag concentration, was calculated. In the influent, an
33 394 average concentration of 3.00 mg/L was determined, in the effluent 2.75 mg/L, and in river
34 395 water 3.16 mg/L. These concentrations correlate to the expected values. Please be aware that
35 396 all water samples were spiked with AgNPs in order to demonstrate the feasibility of the
36 397 method.

37
38 398

39
40 399 **Stability monitoring**

41
42 400 The impacts of engineered nanoparticles on the aquatic environment are dependent on their
43 401 long-term stability. Several previous studies have shown that the stability of AgNPs in
44 402 suspension is highly dependent on the ambient conditions, including the pH, as well as the
45 403 concentration of chloride and dissolved organic matter.³³⁻³⁶

1
2
3 404 With previous long-term studies of the fate of nanoparticles in suspension conducted using
4 405 spICP-MS, laborious preparation of external standards was necessary. Here, the rapid
5 406 monitoring of AgNP diameters by means of spICP-MS with isotope dilution is presented.

6
7
8 407 Figure 4 shows the diameters of the AgNPs stored under different conditions and changes
9 408 over time. For comparison, the nanoparticle size was determined by external calibration and
10 409 with internal calibration based on isotope spiking, as described above.

11 410 In all samples, a decrease of diameter was observed over time (Figure 4). This is most likely
12 411 due to dissolution. An increase in the constant signal resulting from dissolved silver supports
13 412 this assumption.

14 413 As can be clearly seen from sample 2, storage at colder temperatures significantly improves
15 414 the stability (Figure 4). The lowering of pH by the addition of acid, as in sample 3, leads to a
16 415 more rapid decrease in size compared to unaltered purified water (sample 1). These
17 416 observations are in accordance with previous observations.^{33,35}

18 417 Similar diameters were calculated for the AgNPs in the different samples using either daily
19 418 external calibration or internal isotope dilution. These results suggest that internal calibration
20 419 with isotope enriched silver is an excellent strategy to monitor the dissolution of AgNPs in
21 420 aqueous media avoiding laborious and time consuming sample preparation. Only the addition
22 421 of a known amount of isotope enriched silver is necessary. This can be of major importance
23 422 when similar studies are carried out over a period of many days.
24 423

25 424 **Conclusions**

26 425
27 426 This new approach for calculating the diameter of nanoparticles is based on isotope dilution
28 427 analysis with addition of isotope enriched material. Using this analytical method, we were
29 428 able to accurately estimate the mean particle diameter of AgNP suspensions prepared in
30 429 purified water, river water and wastewater, with RSDs of replicate measurements below
31 430 1.9%. There was excellent agreement between the analytical results using this new calibration
32 431 method and the conventional procedure. This method has the advantage of avoiding time-
33 432 consuming preparation of samples and measurement of external standard solutions. In
34 433 addition, matrix effects are overcome when using internal calibration with isotope dilution.
35 434 This is especially crucial when characterizing nanoparticles in complex environmental
36 435 samples. The sample preparation is easy and only needs the addition of the isotope enriched
37 436 standard. This new characterization procedure is ideal for long-term fate studies that require
38 437 the analysis of samples on many different days. Using this method, we were able to
39
40
41
42
43
44
45
46
47
48
49
50
51
52
53
54
55
56
57
58
59
60

1
2
3 438 demonstrate reductions in the size of AgNPs in aqueous suspensions over time as a result of
4 439 dissolution of the core material.

5
6 440 The presented method allows rapid size determination of suspensions of NPs with a distinct
7 441 size. However, it is difficult to investigate complex size distributions. Although this is a
8 442 disadvantage compared to established methods, the new presented method will be of great
9 443 benefit for the analysis of matrix loaded environmental samples and stability experiments that
10 444 focus on NPs with definite diameters.
11
12
13
14
15

16 446 **Acknowledgements**

17 447
18
19 448 This work was supported by a Strategic Research Grant from the Natural Sciences and
20 449 Engineering Research Council (NSERC) of Canada to HH and CDM. LT thanks the German
21 450 Research Foundation (DFG, Bonn, Germany) for financial support in the form of a research
22 451 fellowship. The authors thank Li Shen from McGill University for TEM measurements.
23 452 Funding for this study was provided by NSERC through a Strategic Grant to Prof. Viviane
24 453 Yargeau, (PI), Department of Chemical Engineering, McGill University and her colleagues at
25 454 Trent University (C. Metcalfe) and Laval University (P. Vanrolleghem).
26
27
28
29
30
31
32

33 456 **References**

- 34
35 457 1 B. Wiley, Y.G. Sun, B. Mayers and Y.N. Xia, *Chem.-Eur. J.*, 2005, **11**, 454-463.
36 458 2T. M. Benn and P. Westerhoff, *Environ. Sci. Technol.*, 2008, **42**, 4133-4139.
37 459 3L. Li, G. Hartmann, M. Döblinger and M. Schuster, *Environ. Sci. Technol.*, 2013, **47**, 7317-
38 460 7323.
39 461 4 R. Kaegi, A. Voegelin, B. Sinnet, S. Zuleeg, H. Hagendorfer, M. Burkhardt and H. Siegrist,
40 462 *Environ. Sci. Technol.*, 2011, **45**, 3902-3908.
41 463 5 R. Kaegi, A. Voegelin, C. Ort, B. Sinnet, B. Thalmann, J. Krismer, H. Hagendorfer, M.
42 464 Elumeluand E. Mueller, *Water Res.*, 2013, **47**, 3866-3877.
43 465 6 M. A. Kiser, D. A. Ladner, K. D. Hristovski and P. K. Westerhoff, *Environ. Sci. Technol.*,
44 466 2012, **46**, 7046-7053.
45 467 7 Y. Yin, J. Liu and G. Jiang, *ACS Nano*, 2012, **6**, 7910-7919.
46 468 8 B. Nowack, J. F. Ranville, S. Diamond, J.A. Gallego-Urrea, C. Metcalfe, J. Rose, N. Horne,
47 469 A. A. Koelmans, S. J. Klaine, *Environ. Toxicol. Chem.*, 2012, **31**, 52-59.
48 470 9 K. B. Narayanan, H. H. Park and N. Sakthivel, *Spectrochim. Acta A*, 2013, **116**, 485-490.
49 471 10 S. Ashokkumar, S. Ravi and S. Velmurugan, *Spectrochim. Acta A*, 2013, **115**, 388-392.
50
51
52
53
54
55
56
57
58
59
60

- 1
2
3 472 11 M. Hadioui, S. Leclerc and K.J. Wilkinson, *Talanta*, 2013, **105**, 15-19.
4
5 473 12 M. E. Hoque, K. Khosravi, K. Newman and Chris. D. Metcalfe, *J. Chromatogr. A.*, 2013,
6 474 **1233**, 109-115.
7
8 475 13 M. Delay, T. Dolt, A. Woellhaf, R. Sembritzki and F. H. Frimmel, *J. Chromatogr. A.*,
9 476 2011, **1218**, 4206-4212.
10
11 477 14 E. Bolea, J. Jiménez-Lamana, F. Laborda and J. R. Castillo, *Anal. Bioanal. Chem.*, 2011,
12 478 **401**, 2723-2732.
13
14 479 15 J. Soto-Alvaredo, M. Montes-Bayón and J. Bettmer, *Anal. Chem.*, 2013, **85**, 1316-1321.
15
16 480 16 C. Degueldre and P.-Y. Favarger, *Colloid. Surface. A*, 2003, **217**, 137-142.
17
18 481 17 C. Degueldre and P.-Y. Favarger, *Talanta*, 2004, **62**, 1051-1054.
19
20 482 18 C. Degueldre, P.-Y. Favarger and C. Bitea, *Anal. Chim. Acta*, 2004, **518**, 137-142.
21
22 483 19 C. Degueldre, P.-Y. Favarger and S. Wold, *Anal. Chim. Acta*, 2006, 555, 263-268.
23
24 484 20 S. Gschwind, L. Flamigni, J. Koch, O. Borovinskaya, S. Groh, K. Niemax and D. Günther,
25 485 *J. Anal. Atom. Spectrom.*, 2011, **26**, 1166-1174.
26
27 486 21 F. Laborda, J. Jiménez-Lamana, E. Bolea and J. R. Castillo, *J. Anal. Atom. Spectrom.*,
28 487 2011, **26**, 1362-1371.
29
30 488 22 D. M. Mitrano, E. K. Lesher, A. Bednar, J. Monserud, C. P. Higgins and J. F. Ranville,
31 489 *Environ. Toxicol. Chem.*, 2012, **31**, 115-121.
32
33 490 23 H. E. Pace, N. J. Rogers, C. Jarolimek, V. A. Coleman, C. P. Higgins and J. F. Ranville,
34 491 *Anal. Chem.*, 2011, **83**, 9361-9369.
35
36 492 24 S. A. Pergantis, T. L. Jones-Lepp and E. M. Heithmar, *Anal. Chem.*, 2012, **84**, 6454-6462.
37
38 493 25 B. Franze, I. Strenge and C. Engelhard, *J. Anal. Atom. Spectrom.*, 2012, **27**, 1074-1082.
39
40 494 26 J. Tuoriniemi, G. Cornelis and M. Hassellöv, *Anal. Chem.*, 2012, **84**, 3965-3972.
41
42 495 27 R. B. Reed, C. P. Higgins, P. Westerhoff, S. Tadjiki and J. F. Ranville, *J. Anal. Atom.*
43 496 *Spectrom.*, 2012, **27**, 1093-1100.
44
45 497 28 D. M. Mitrano, A. Barber, A. Bednar, P. Westerhoff, C. P. Higgins and J. F. Ranville, *J.*
46 498 *Anal. Atom. Spectrom.*, 2012, **27**, 1131-1142.
47
48 499 29 H. E. Pace, N. J. Rogers, C. Jarolimek, V. A. Coleman, E. P. Gray, C. P. Higgins and J. F.
49 500 Ranville, *Environ. Sci. Technol.*, 2012, **46**, 12272-12280.
51
52 501 30 F. Laborda, J. Jiménez-Lamana, E. Bolea and J. R. Castillo, *J. Anal. Atom. Spectrom.*,
53 502 2013, **28**, 1220-1232.
54
55 503 31 K. Loeschner, J. Navratilova, C. Købler, K. Mølhav, S. Wagner, F. von der Kammer and
56 504 E. H. Larsen, *Anal. Bioanal. Chem.*, 2013, **405**, 8185-8195.
57
58
59
60

- 1
2
3 505 32 P. Rodríguez-González, J. M. Marchante-Gayón, J. I. G. Alonso and A. Sanz-Medel,
4 506 *Spectrochim. Acta B*, 2005, **60**, 151-207.
5
6 507 33 S. Elzey, V. H. Grassian, *J. Nanopart. Res.*, 2010, **12**, 1945-1958.
7
8 508 34 A. J. Kennedy, M. A. Chappell, A. J. Bednar, A. C. Ryan, J. G. Laird, J. K. Stanley, J. A.
9 509 Steevens, *Environ. Sci. Technol.*, 2012, **46**, 10772 - 10780.
10
11 510 35 S. K. Misra, A. Dybowska, D. Berhanu, S. N. Luoma, E. Valsami-Jones, *Sci. Total*
12 511 *Environm.*, 2012, **438**, 225-232.
13
14 512 36 X. Li, J. J. Lenhart, H. W. Walker, *Langmuir*, 2012, **28**, 1095-1104.
15
16 513
17
18
19
20
21
22
23
24
25
26
27
28
29
30
31
32
33
34
35
36
37
38
39
40
41
42
43
44
45
46
47
48
49
50
51
52
53
54
55
56
57
58
59
60

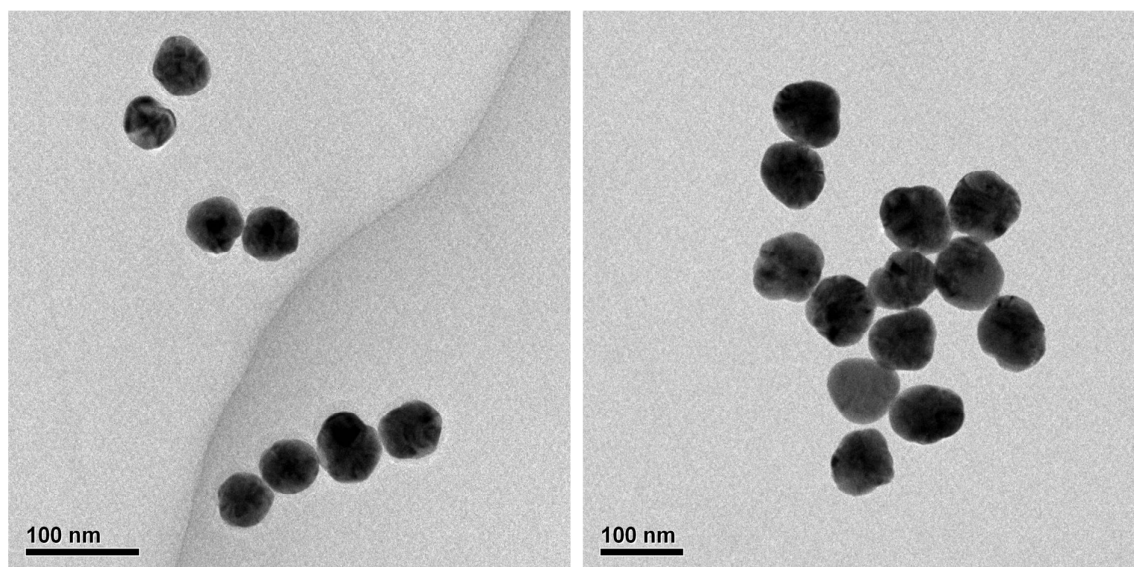
514 **Figure Captions**

515

516 Figure 1: TEM photomicrographs of AgNPs with nominal diameters of 50 nm (left) and 80
517 nm (right).

518

519



520

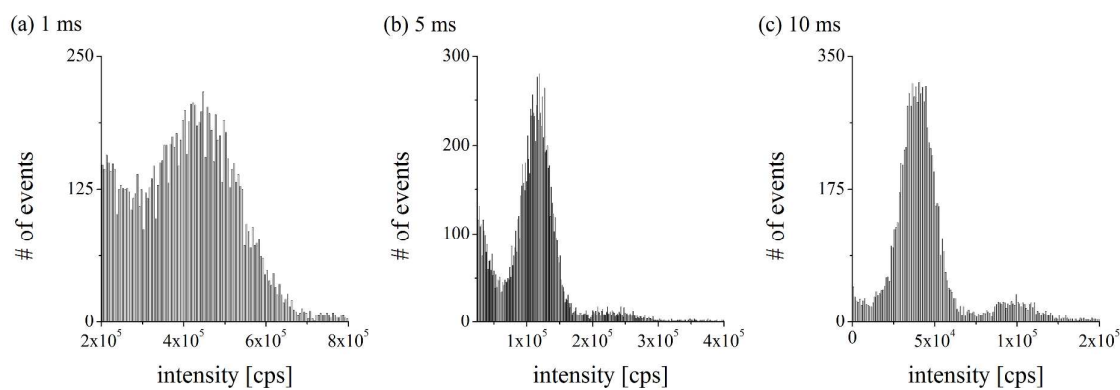
521

522

523

524 Figure 2: Histograms of the peak intensity of 80 nm PVP capped AgNPs run with dwell times
525 of (a) 1 ms, (b) 5 ms, and (c) 10 ms.

526



527

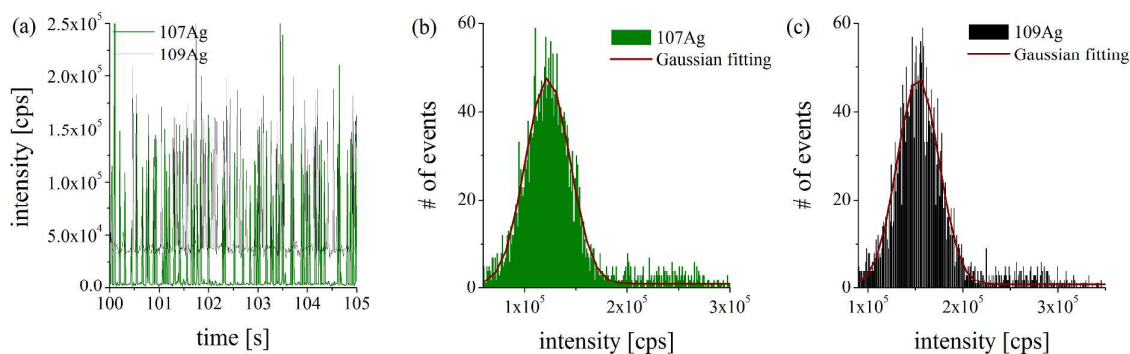
528

529

530

531 Figure 3: Transient signal and histograms of the peak intensity of both silver isotopes of 80
 532 nm PVP capped AgNPs run in sp mode.

533

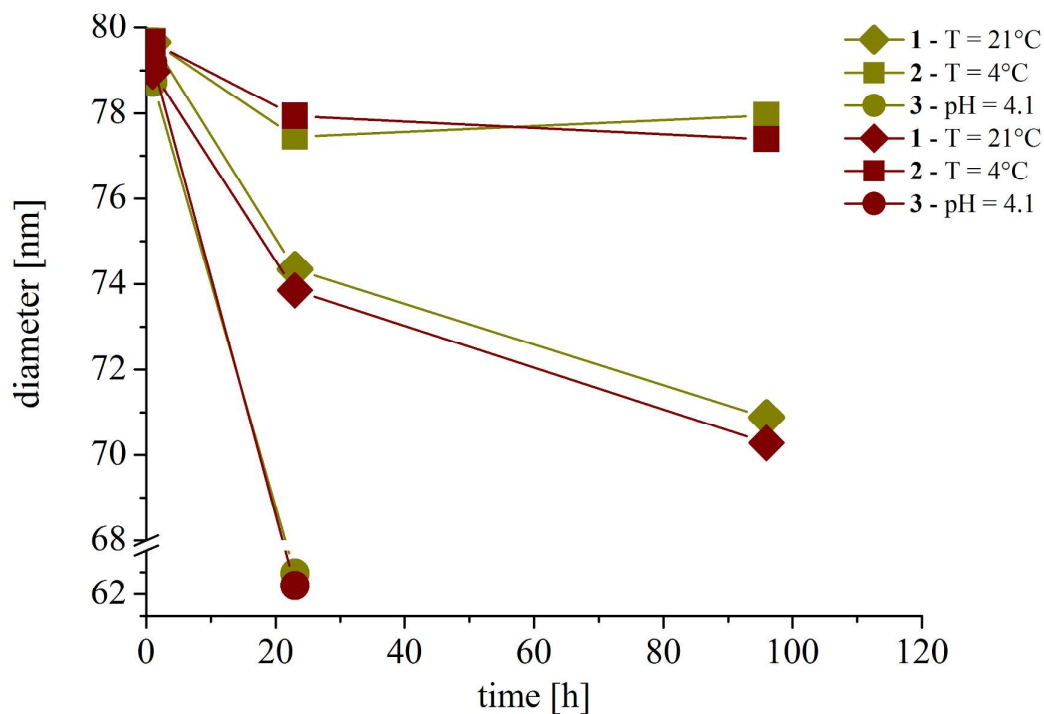


534

535

536 Figure 4: Changes in the mean diameter of AgNPs in suspension over time under different
 537 storage conditions. Results of sizing with internal isotope dilution are shown in green, and the
 538 sizing using external calibration in brown.

539



540

541

542 **Tables**

543

544 Table 1: Mean diameters and relative standard deviations (RSD) of AgNPs suspended in
 545 water, determined with internal calibration with a ^{109}Ag enriched isotope and with
 546 conventional external calibration.

547

	50 nm, citrate capped		80 nm, PVP capped	
Internal calibration				
Mean diameter	50.16 nm	51.07 nm	80.20 nm	79.85 nm
<i>RSD</i>	1.51%	1.31%	1.28%	1.45%
External calibration				
Mean diameter	50.40 nm	50.89 nm	79.70 nm	79.06 nm
<i>RSD</i>	1.14%	1.14%	0.23%	1.28%

548

549

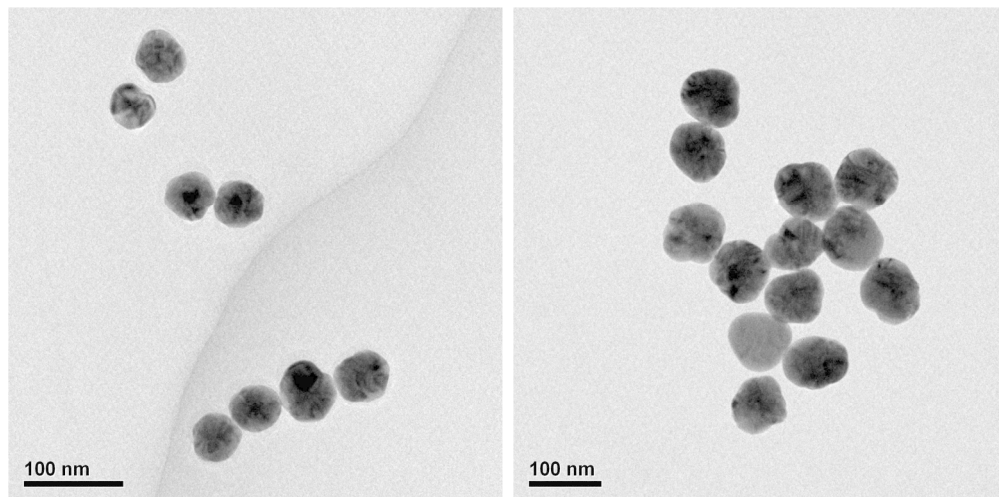
550 Table 2: Mean diameters and relative standard deviations (RSD) of AgNPs in spiked samples
 551 of wastewater influent and effluent, and river water, determined by internal calibration with a
 552 ^{109}Ag enriched isotope.

553

	Influent	Effluent	River water
Mean diameter	79.96 nm	80.22 nm	78.79 nm
<i>RSD</i>	1.90%	1.17%	0.74%

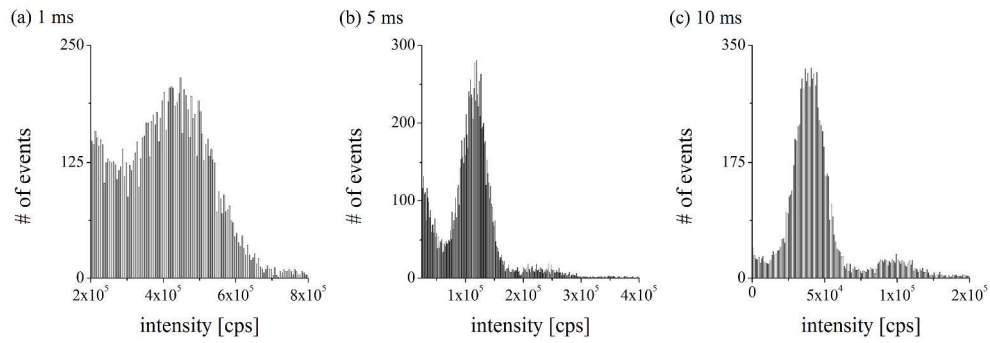
554

1
2
3
4
5
6
7
8
9
10
11
12
13
14
15
16
17
18
19
20
21
22
23
24
25
26
27
28
29
30
31
32
33
34
35
36
37
38
39
40
41
42
43
44
45
46
47
48
49
50
51
52
53
54
55
56
57
58
59
60

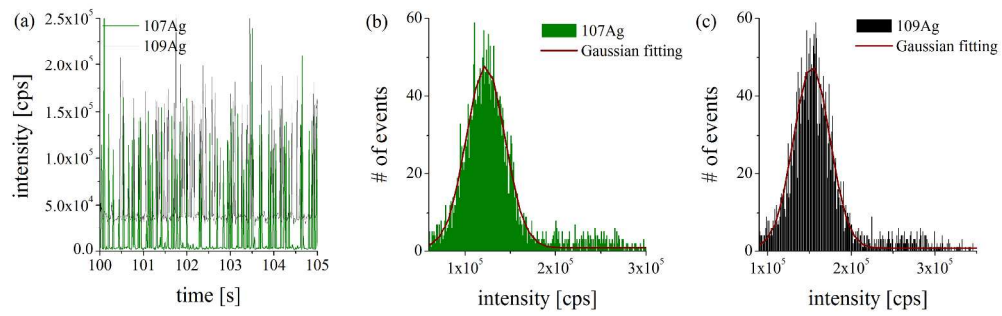


385x190mm (150 x 150 DPI)

1
2
3
4
5
6
7
8
9
10
11
12
13
14
15
16
17
18
19
20
21
22
23
24
25
26
27
28
29
30
31
32
33
34
35
36
37
38
39
40
41
42
43
44
45
46
47
48
49
50
51
52
53
54
55
56
57
58
59
60

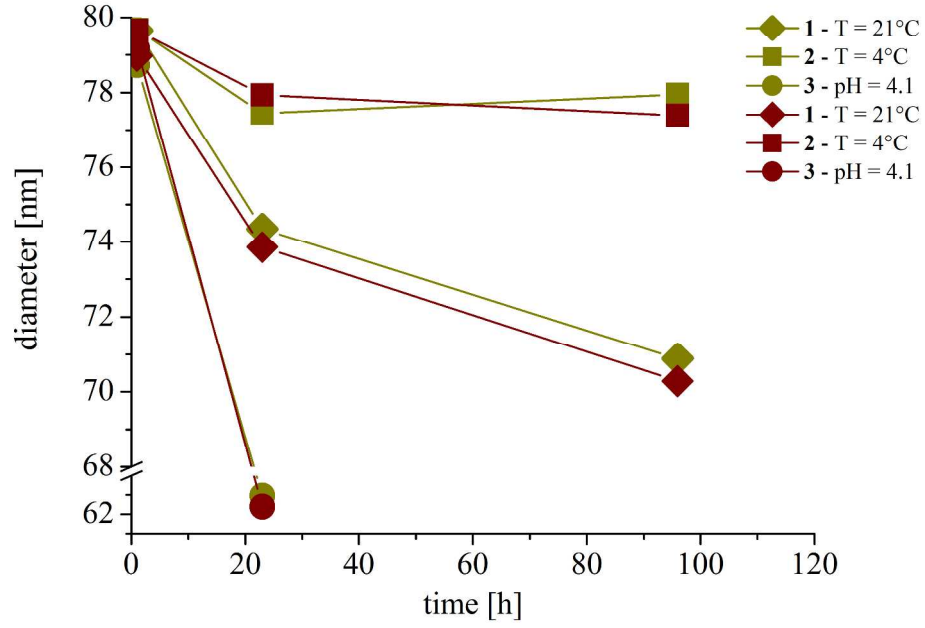


359x119mm (300 x 300 DPI)



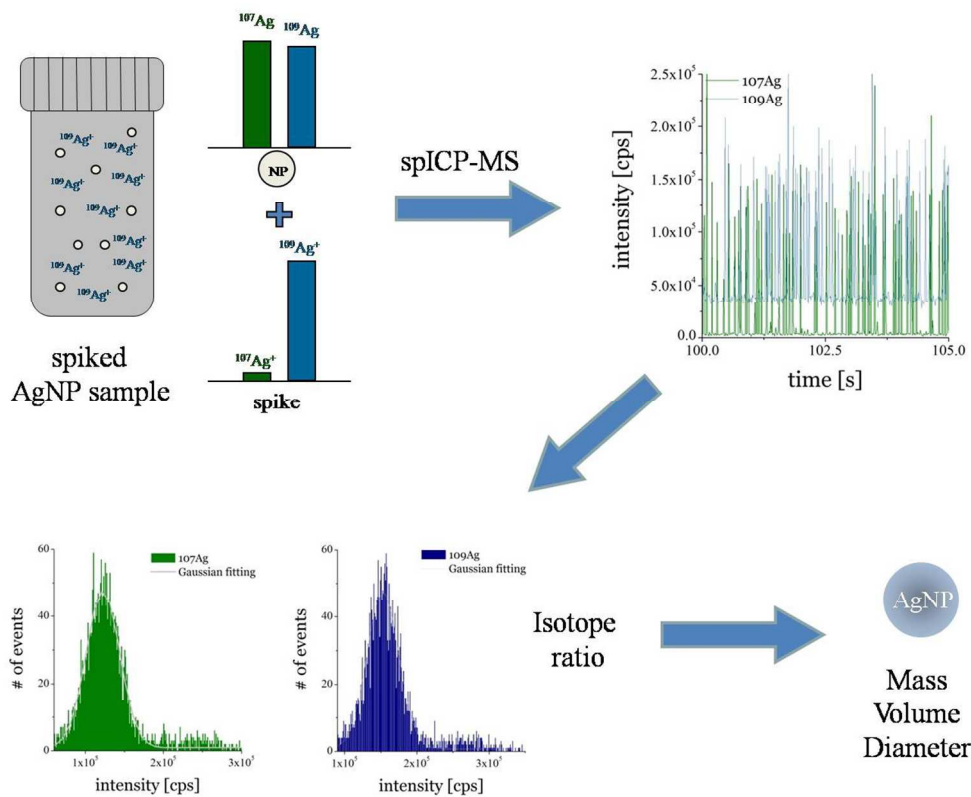
359x119mm (300 x 300 DPI)

1
2
3
4
5
6
7
8
9
10
11
12
13
14
15
16
17
18
19
20
21
22
23
24
25
26
27
28
29
30
31
32
33
34
35
36
37
38
39
40
41
42
43
44
45
46
47
48
49
50
51
52
53
54
55
56
57
58
59
60



281x202mm (300 x 300 DPI)

1
2
3
4
5
6
7
8
9
10
11
12
13
14
15
16
17
18
19
20
21
22
23
24
25
26
27
28
29
30
31
32
33
34
35
36
37
38
39
40
41
42
43
44
45
46
47
48
49
50
51
52
53
54
55
56
57
58
59
60



224x178mm (150 x 150 DPI)